

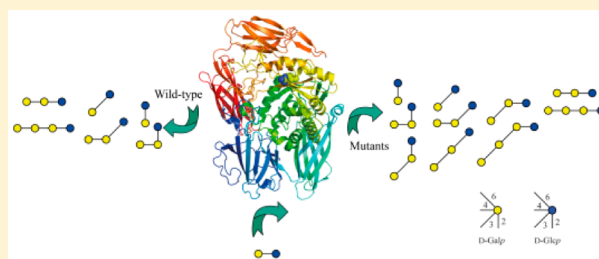
# Engineering of the *Bacillus circulans* $\beta$ -Galactosidase Product Specificity

Huifang Yin,<sup>†</sup> Tjaard Pijning,<sup>§</sup> Xiangfeng Meng,<sup>†</sup> Lubbert Dijkhuizen,<sup>\*,†</sup> and Sander S. van Leeuwen<sup>†</sup>

<sup>†</sup>Microbial Physiology and <sup>§</sup>Biophysical Chemistry, Groningen Biomolecular Sciences and Biotechnology Institute (GBB), University of Groningen, Nijenborgh 7, 9747 AG Groningen, The Netherlands

## Supporting Information

**ABSTRACT:** Microbial  $\beta$ -galactosidase enzymes are widely used as biocatalysts in industry to produce prebiotic galactooligosaccharides (GOS) from lactose. GOS mixtures are used as beneficial additives in infant formula to mimic the prebiotic effects of human milk oligosaccharides (hMOS). The structural variety in GOS mixtures is significantly lower than in hMOS. Since this structural complexity is considered as the basis for the multiple biological functions of hMOS, it is important to broaden the variety of GOS structures. In this study, residue R484 near +1 subsite of the C-terminally truncated  $\beta$ -galactosidase from *Bacillus circulans* (BgaD-D) was subjected to site saturation mutagenesis. Especially the R484S and R484H mutant enzymes displayed significantly altered enzyme specificity, leading to a new type of GOS mixture with altered structures and linkage types. The GOS mixtures produced by these mutant enzymes contained 14 structures that were not present in the wild-type enzyme GOS mixture; 10 of these are completely new structures. The GOS produced by these mutant enzymes contained a combination of  $(\beta 1 \rightarrow 3)$  and  $(\beta 1 \rightarrow 4)$  linkages, while the wild-type enzyme has a clear preference toward  $(\beta 1 \rightarrow 4)$  linkages. The yield of the trisaccharide  $\beta$ -D-Galp-(1  $\rightarrow$  3)- $\beta$ -D-Galp-(1  $\rightarrow$  4)-D-Glcp produced by mutants R484S and R484H increased 50 times compared to that of the wild-type enzyme. These results indicate that residue R484 is crucial for the linkage specificity of BgaD-D. This is the first study showing that  $\beta$ -galactosidase enzyme engineering results in an altered GOS linkage specificity and product mixture. The more diverse GOS mixtures produced by these engineered enzymes may find industrial applications.



Prebiotics are nondigestible food ingredients that selectively stimulate the growth or activity of specific bacterial species in the colon, thereby beneficially affecting the colonic microbiota and improving the host health.<sup>1</sup> Galactooligosaccharides (GOS) have drawn a great deal of attention in the field of prebiotics because they have been shown to significantly modulate the species composition of colonic microbiota.<sup>2</sup> GOS are added in infant formula to mimic the molecular size and prebiotic benefits of hMOS.<sup>3,4</sup> Numerous studies have shown that GOS greatly increased the number of Bifidobacteria and their metabolic activity in the gut,<sup>5–8</sup> reduced the incidence of allergy,<sup>9,10</sup> reduced adhesion of pathogens,<sup>11</sup> and mediated the gut immune system.<sup>6,10,12</sup> Moreover, GOS are effective in the treatment of metabolic diseases.<sup>13</sup>

GOS are oligosaccharides that consist of a number of galactose units linked to a terminal glucose or galactose residue via different glycosidic bonds, with degrees of polymerization (DP) from 2 to 10 units.<sup>14,15</sup> Microbial  $\beta$ -galactosidase enzymes are widely used as biocatalysts in industry to produce GOS.<sup>5</sup> The formation of GOS proceeds via a double displacement mechanism (Figure 1). The catalytic nucleophile first attacks the anomeric center of lactose, forming a galactosyl-enzyme intermediate while releasing glucose. The second step depends on the identity of the acceptor substrate: if water serves as the acceptor, the intermediate undergoes hydrolysis and releases galactose; if lactose serves as acceptor substrate, a

DP3 GOS ( $\beta$ -D-Galp-(1  $\rightarrow$  x)- $\beta$ -D-Galp-(1  $\rightarrow$  4)-D-Glcp) is formed by transgalactosylation.<sup>16–21</sup> This DP3 GOS may serve again as acceptor substrate and undergo another round of transgalactosylation. The transgalactosylation reaction thus results in GOS mixtures containing different structures.

Rodriguez-Colinas et al. identified five structures in the GOS mixture produced by  $\beta$ -galactosidase from *Kluyveromyces fragilis*.<sup>22</sup> Urrutia et al. found nine structures in the GOS mixture produced by  $\beta$ -galactosidase from *Aspergillus oryzae*.<sup>23</sup> Yanahira et al. isolated 11 GOS structures from the products of  $\beta$ -galactosidase of *Bacillus circulans*.<sup>24</sup> We identified 43 structures in the commercial Vivinal GOS produced with  $\beta$ -galactosidase of *B. circulans*.<sup>25,26</sup> Recently we compared 6 commercial GOS products with Vivinal GOS and found 13 new structures.<sup>27</sup> Taken together, a total of 60 structures have been characterized in the GOS produced by various  $\beta$ -galactosidase enzymes. However, the structure and linkage variability in these GOS mixtures is far less than that of human milk oligosaccharides (hMOS) structures.<sup>28</sup> The structural complexity of hMOS is considered as the basis for their multiple biological functions.<sup>29</sup> We therefore studied the synthesis of GOS mixtures with enhanced structural variety.

Received: January 16, 2017

Published: January 16, 2017

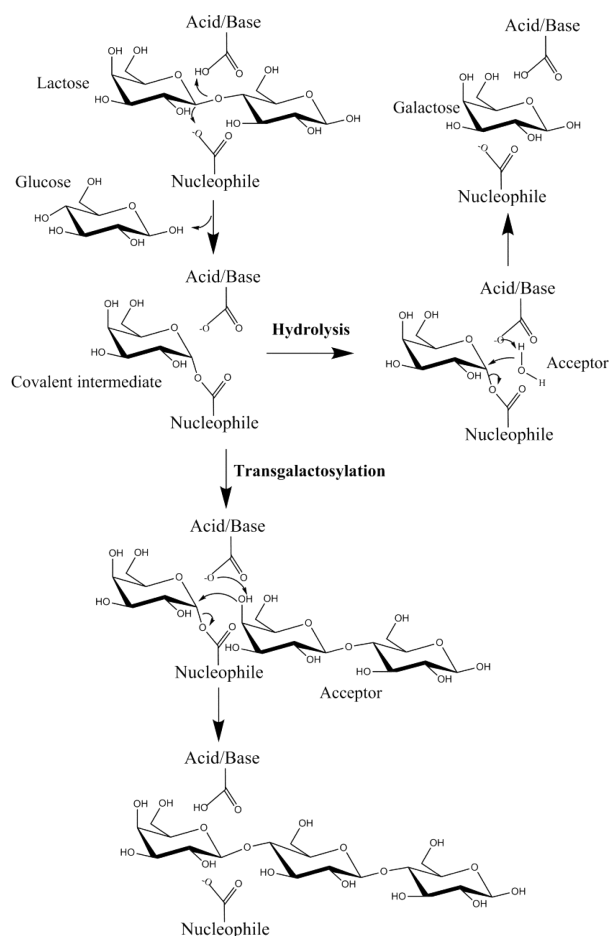


**Figure 1.** Reaction scheme of  $\beta$ -galactosidase enzymes. This figure has been adapted from Bultema et al.<sup>6</sup> In *B. circulans*  $\beta$ -galactosidase, the nucleophile is E532, the acid/base catalyst is E447. The hydrolysis reaction uses water as acceptor substrate, while the transgalactosylation reaction uses lactose and other carbohydrates as acceptor substrate.

At present it is unknown what features in  $\beta$ -galactosidase proteins determine the structural and linkage diversity of their GOS product mixtures. Previously we have shown that in

glucanucrase enzymes residues near the acceptor binding site play important roles in the linkage and reaction specificity.<sup>30,31</sup> Site saturation mutagenesis was performed on the R484 residue of BgaD-D to elucidate its role in determining enzyme specificity and the effects of mutagenesis on products synthesized, since it is close to the +1 acceptor subsite (Figure 2) in both *B. circulans*  $\beta$ -galactosidase (PDB ID: 4YPJ) and  $\beta$ -galactosidase from *Streptococcus pneumoniae* (PDB ID: 4CUC).<sup>32,33</sup> Mutant enzymes showing altered product specificity were studied in more detail, and their GOS mixtures were characterized. MALDI-TOF-MS, NMR spectroscopy, and HPAEC-PAD profiling revealed that these GOS mixtures mainly contained ( $\beta$ 1  $\rightarrow$  3) and ( $\beta$ 1  $\rightarrow$  4) linkages, which is different from any known commercial GOS products. Their structural characterization resulted in the identification of 14 new GOS compounds, thus greatly enriching the currently available GOS variety.

## EXPERIMENTAL SECTION

**Plasmid Construction and Mutagenesis.** The C-terminally truncated *B. circulans*  $\beta$ -galactosidase (BgaD-D) protein was used as wild type enzyme in this study.<sup>16,17,34,35</sup> PCR amplification was performed in order to add a 6 $\times$  His tag at the N-terminus of BgaD-D. The template was plasmid pET-15b containing the BgaD-D encoding gene.<sup>16</sup> A forward primer (5'-CAGGGACCCGGTATG GGAAACAGTGTGAGC-3') and reverse primer (5'-CGAGGAGAAGCCCGGTTATG-GCGTTACCGTAAATAC-3') were used for PCR amplification; the PCR product was purified on an agarose gel. Vector pET-15b-LIC was digested by FastDigest *KpnI* (Thermo Scientific) and purified with a PCR purification kit (GE Healthcare). Subsequently, the PCR product was treated with T4 DNA polymerase (New England BioLabs) in the presence of 2.5 mM dATP, while the vector was digested with T4 DNA polymerase in the presence of 2.5 mM dTTP. Both reactions were incubated at room temperature for 60 min, followed by 20 min at 75  $^{\circ}$ C to inactivate the enzymes. The reaction mixture containing 2  $\mu$ L of the target DNA and 1  $\mu$ L vector was incubated at room temperature for 15 min to allow ligation. Then the mixture was transformed into *Escherichia coli* DH5 $\alpha$  competent cells (Phabagen). The DNA sequence was verified

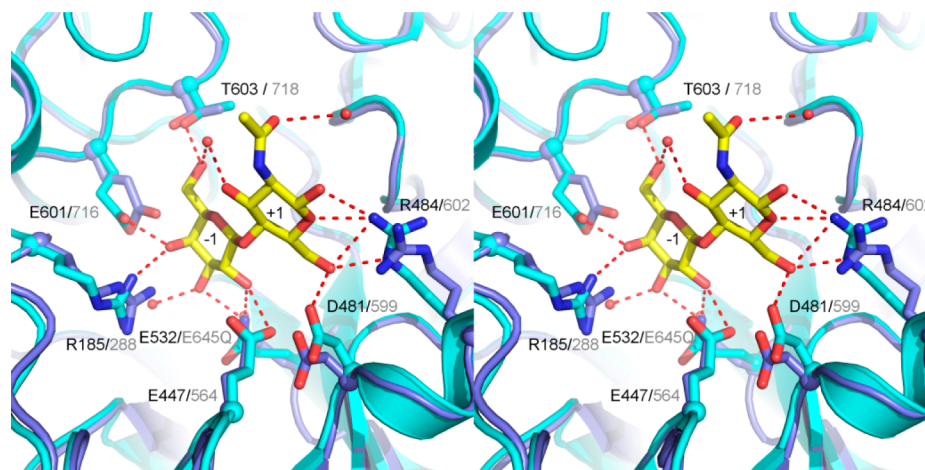


**Figure 2.** Stereoview of the active site of two  $\beta$ -galactosidase structures: BgaD-D (PDB entry 4YPJ, blue) superimposed with the nucleophile mutant (E645Q) of  $\beta$ -galactosidase from *Streptococcus pneumoniae* in complex with LacNAc (PDB entry 4CUC, cyan). The two enzymes share 49% sequence identity. R602 in 4CUC (corresponding to R484 in 4YPJ) interacts with the LacNAc (yellow carbon atoms) in the +1 subsite; hydrogen bond interactions are shown as red dashed lines. Residues of 4YPJ are labeled in black, and the residues of 4CUC are labeled in gray.

by sequencing. Then the plasmid pET-15b-LIC containing the BgaD-D gene was used as the template for site-directed mutagenesis. Mutations at R484 were introduced by various primers (Supporting Information Table 1) using the

**Table 1. Kinetic Properties of *B. circulans*  $\beta$ -Galactosidase Wild-Type BgaD-D and Mutants Derived**

enzyme <sup>a</sup>	$K_m$ mM	$k_{cat}$ s <sup>-1</sup>	$k_{cat}/K_m$ s <sup>-1</sup> M <sup>-1</sup>
WT	112.9 ± 12.7	199.8 ± 5.3	1770
R484S	95.4 ± 7.7	119.1 ± 5.1	1250
R484H	151.3 ± 9.4	148.8 ± 4.3	980
R484G	161.3 ± 3.5	179.8 ± 2.5	1110
R484N	133.3 ± 6.7	153.9 ± 2.9	1150
R484C	130.2 ± 3.6	107.7 ± 0.9	830

<sup>a</sup>Kinetic parameters were determined with 10 different lactose concentrations ranging from 10 to 500 mM.

QuikChange site-directed mutagenesis kit (Stratagene). The PCR product was digested by FastDigest DpnI (Thermo Fisher) and cleaned up with a PCR purification kit. The cleaned PCR product was transformed into *E. coli* BL21 (DE3) (Invitrogen). After growth on LB agar (containing 100  $\mu$ g/mL ampicillin), 20 colonies were randomly selected and inoculated into 10 mL of LB medium containing 100  $\mu$ g/mL ampicillin for overnight growth at 37 °C. Plasmid DNA of the overnight cultures was isolated using a miniprep kit (Sigma-Aldrich) for nucleotide sequencing.

**Enzyme Production and Purification.** The wild-type BgaD-D enzyme and mutant proteins were heterologously produced and purified. Briefly, the plasmids containing the wild-type and mutant genes were transferred into *E. coli* BL21 (DE3) competent cells. After growth on LB agar plates (containing 100  $\mu$ g/mL ampicillin), colonies were inoculated for overnight cultivation. Then 1% overnight culture was inoculated into fresh LB medium (containing 100  $\mu$ g/mL ampicillin) and incubated at 37 °C. When the cell density reached about 0.6 at 600 nm, expression of the recombinant proteins was induced with 1 mM isopropyl- $\beta$ -D-thiogalactopyranoside. Subsequently, the cells were cultured overnight at 30 °C and harvested by centrifugation. Cell pellets were washed with 20 mM Tris-HCl buffer (pH 8.0) and lysed with B-PER lysis solution (Thermo Scientific) for 1 h at room temperature. The cell debris was removed by centrifugation. The supernatant was mixed with HIS-Select Nickel Affinity Gel and incubated at 4 °C overnight. Unbound proteins were washed away with 20 mM Tris-HCl (pH 8.0), 50 mM NaCl (buffer A); the recombinant proteins were eluted with buffer A containing 100 mM imidazole. Then imidazole was removed by ultra-centrifugation with a cutoff of 30 kDa (Merck).

**Enzyme Activity Assays.** Activity assays were performed with 0.5 mg/mL enzymes with 10% (w/w) lactose in 100 mM sodium phosphate buffer, pH 6.0, at 40 °C. Samples of 100  $\mu$ L incubation mixture were withdrawn every minute for 5 min and inactivated with 50  $\mu$ L of 1.5 M NaOH. After 10 min the samples were neutralized with 50  $\mu$ L of 1.5 M HCl. The released glucose was measured using a D-glucose assay kit (GOPOD Format). One unit of total enzyme activity was defined as the release of 1  $\mu$ mol of glucose per min. The kinetic parameters ( $K_m$  and  $k_{cat}$ ) were determined with 10 different lactose concentrations ranging from 10 to 500 mM. The kinetic parameters were determined with OriginPro 9.0 software (OriginLab).

**Enzymatic Production of GOS.** For the production of GOS, wild-type BgaD-D and R484 mutant enzymes (3.75 units/mL) were incubated with 50% (w/w) lactose in 100 mM sodium phosphate buffer, pH 6.0, for 20 h at 60 °C to reach the highest GOS yield. The enzymes were inactivated by incubation at 100 °C for 10 min.

**HPAEC-PAD Analysis and Quantification of GOS.** The GOS produced by the wild-type BgaD-D and mutant enzymes were diluted 1000 times with Milli-Q water, and analyzed and quantified by high performance anion exchange chromatography (HPAEC) on a Dionex ICS-3000 workstation, equipped with an ICS3000 pulsed amperometric detector (PAD). GOS were separated on a CarboPac PA1 analytical column (2 × 250 mm) by using an adapted gradient based on previously described separation conditions for (4 × 250 mm) columns (Supporting Information, Figure S1).<sup>36</sup> A calibration curve of lactose, galactose, and glucose ranging from 10 to 1000  $\mu$ M was used for the quantification of GOS yield (GOS yield (g) = initial lactose (g) - [remaining lactose (g) + galactose (g) + glucose (g)] after 20 h). A calibration curve ranging from 4 to 200  $\mu$ g/mL was used for the quantification of  $\beta$ -D-Galp-(1 → 3)- $\beta$ -D-Galp-(1 → 4)-D-Glcp (Sigma). Because of a lack of calibration references for  $\beta$ -D-Galp-(1 → 3)- $\beta$ -D-Glcp,  $\beta$ -D-Galp-(1 → 2)- $\beta$ -D-Glcp,  $\beta$ -D-Galp-(1 → 4)- $\beta$ -D-Galp-(1 → 4)-D-Glcp,  $\beta$ -D-Galp-(1 → 4)- $\beta$ -D-Galp-(1 → 3)-D-Glcp and  $\beta$ -D-Galp-(1 → 4)- $\beta$ -D-Galp-(1 → 2)-D-Glcp, the yield of these compounds were estimated by comparing the peak intensities in HPAEC-PAD profiles.

**Separation and Identification of GOS Fractions.** GOS produced by the R484S mutant enzyme were loaded onto Extract Clean Carbograph Columns (Grace Davison Discovery Sciences) to remove salt and monosaccharides. The GOS mixtures were fractionated using a CarboPac PA1 Semi-Preparative column (9 × 250 mm) on a Dionex ICS-5000 workstation (separation conditions, see Supporting Information, Figure S1). The separated GOS fractions were manually collected, exchanged, and lyophilized twice with 99.9%<sub>atom</sub> D<sub>2</sub>O (Cambridge Isotope Laboratories). Samples were dissolved in 650  $\mu$ L of 99.9%<sub>atom</sub> D<sub>2</sub>O, containing 25 ppm acetone ( $\delta^1\text{H}$  2.225,  $\delta^{13}\text{C}$  31.08) as an internal standard. All spectra were recorded with a <sup>1</sup>H spectral width of 4800 Hz, and where applicable 10 000 Hz for <sup>13</sup>C spectra. 1D 600-MHz <sup>1</sup>H NMR spectra were recorded with 16k complex data points, using a WET1D pulse for HOD signal suppression. 2D COSY spectra were recorded in 200 increments of 4000 complex points. 2D TOCSY spectra were recorded in 200 increments of 2000 complex data points, using MLEV17 pulse of 50 and 150 ms spin-lock times. 2D <sup>13</sup>C-<sup>1</sup>H HSQC spectra were recorded using 2000 complex data points with 128 increments. 2D ROESY spectra with 300 ms mixing time were recorded in 200 increments of 2000 complex data points. All spectra were processed using MestReNova 5.3 (Mestrelabs Research SL, Santiago de Compostela, Spain), using Whittaker Smoother baseline correction and manual phase correction. The DP of the samples was verified by MALDI-TOF-MS analysis. The samples (1  $\mu$ L) after NMR measurement were mixed with 1  $\mu$ L of 2,5-dihydroxybenzoic acid (10 mg/mL) in 40% (v/v) acetonitrile to allow crystallization. The experiments were performed on an Axima performance mass spectrometer (Shimadzu Kratos Inc.) equipped with a nitrogen laser (337 nm, 3 ns pulse width). Masses were calibrated using an external calibration ladder of DP 1 to 8 malto-oligosaccharides. Peak



positions were confirmed by reinjection on an analytical (2 × 250 mm) CarboPac PA1 column as described above.

## RESULTS

**Cloning, Production, and Purification of Wild-type BgaD-D and R484 Mutants.** Site saturation mutagenesis was performed on residue R484 of BgaD-D to elucidate its role in determining the enzyme product specificity. Mutations in *B. circulans*  $\beta$ -galactosidase were introduced by PCR using the random primers described in the [Experimental Section](#). Six mutant genes of R484 (R484A, R484P, R484Q, R484S, R484L, R484C) were identified in the first round of sequencing. Then the specific primers for the other 13 mutations ([Supporting Information, Table S1](#)) were used for a second round to achieve site saturation mutagenesis at this position. Wild-type BgaD-D and all R484 mutant proteins were produced in *E. coli* BL21 (DE3) and purified. Compared with BgaD-D, no significant differences in expression levels of the mutant proteins were observed ([Supporting Information, Figure S2](#)).

**Effects of Mutations on Kinetic Properties of Enzymes.** The wild-type BgaD-D and mutant enzymes displayed Michaelis–Menten kinetics in the reaction with lactose. The kinetic parameters ( $K_m$  and  $k_{cat}$ ) were determined for the wild-type BgaD-D enzyme and for selected R484 mutants ([Table 1](#)). Compared to the wild-type enzyme, R484S showed a 15.5% decrease in the  $K_m$  value for lactose, while the R484G, R484H, R484N, R484C mutants showed an increase of 16–43% in their  $K_m$  values ([Table 1](#)). Mutant R484G showed only a 10% decrease in  $k_{cat}$  value, whereas the  $k_{cat}$  values of R484S, R484H, R484N, and R484C were reduced to 53.9–77.0% of the wild-type enzyme  $k_{cat}$  ([Table 1](#)). Thus, the catalytic efficiencies ( $K_m/k_{cat}$ ) of the mutants were reduced to 46.9–70.6% ([Table 1](#)). The reduced catalytic efficiencies led to a lower enzyme activity for the mutants compared to the wild-type enzyme ([Table 2](#)).

**Effects of Mutations on Transgalactosylation and Linkage Specificity of GOS.** HPAEC-PAD analysis showed different product profiles for mutant R484S and the BgaD-D wild-type enzyme ([Figure 3A](#)). The products were fractionated on a semipreparative CarboPac PA1 column (9 × 250 mm). Fractions were analyzed by NMR spectroscopy and MALDI-TOF-MS, in order to identify the structures produced. In previous structural studies of GOS, NMR structural-reporter signals have been identified.<sup>25–27</sup> Peaks 1–13, 18, 21–31, and 38 could be assigned based on 1D <sup>1</sup>H NMR spectra, matching those of known structures.<sup>25–27</sup> On the basis of previous data, <sup>1</sup>H and <sup>13</sup>C chemical shift patterns can be recognized for each type of residue.<sup>27</sup> The newly isolated structures 39–46 were studied by MALDI-TOF-MS, 1D and 2D <sup>1</sup>H and <sup>13</sup>C NMR spectroscopy, and reinjected on analytical HPAEC-PAD to verify peak positions. All structures identified are presented in [Figure 3B](#).

A detailed description of the NMR analysis is provided in [Supporting Information](#). The new structures identified showed that the R484S mutant had a novel activity, allowing ( $\beta 1 \rightarrow 3$ ) elongation on galactose residues, whereas the wild-type enzyme only performed ( $\beta 1 \rightarrow 3$ ) substitution on the reducing glucose residue, and has a preference of ( $\beta 1 \rightarrow 4$ ) elongation of Gal. A total of 29 structures were confirmed, including 15 structures found in the wild-type GOS compounds. Besides, 14 structures were identified in the R484S product profile that were absent in the wild-type product profile. Of these compounds, 4 were identified previously in other commercial GOS samples,<sup>27</sup> and

**Table 2. Effects of Mutations of Residue R484 on Enzyme Activity, Transgalactosylation GOS Yield and GOS Linkage Specificity<sup>a</sup>**

enzymes	relative activity <sup>b</sup>	structure 12 yield <sup>c</sup>	GOS yield <sup>d</sup>	structure 12 (%) in total GOS <sup>e</sup>
WT	100	0.2 ± 0.05	63.5 ± 0.8	0.3
R484S	50.5	10.5 ± 1.4	65.0 ± 0.8	16.2
R484H	47.7	10.2 ± 0.5	60.6 ± 0.5	16.9
R484G	66.0	8.7 ± 0.2	59.7 ± 1.5	14.6
R484N	48.3	8.5 ± 0.5	60.8 ± 1.0	13.9
R484C	42.4	7.6 ± 0.3	63.5 ± 1.5	11.9
R484T	39.7	7.2 ± 0.4	65.2 ± 0.7	11.1
R484V	34.7	6.3 ± 0.3	63.2 ± 2.2	9.9
R484A	45.1	6.2 ± 0.1	63.8 ± 0.1	9.8
R484P	24.0	6.2 ± 0.4	59.3 ± 1.7	10.4
R484D	36.5	4.2 ± 0.3	60.1 ± 1.2	7.0
R484I	48.8	3.8 ± 0.1	62.5 ± 0.4	6.1
R484F	28.4	3.2 ± 0.1	61.5 ± 0.9	5.2
R484Q	54.4	2.7 ± 0.7	63.0 ± 0.9	4.2
R484W	17.9	2.7 ± 0.1	57.9 ± 2.0	4.6
R484M	27.3	2.6 ± 0.4	62.9 ± 2.2	4.2
R484E	33.5	2.2 ± 0.2	61.9 ± 0.8	3.6
R484L	38.2	2.2 ± 0.7	59.7 ± 0.1	3.6
R484 K	35.0	1.8 ± 0.1	66.4 ± 0.6	2.7
R484Y	41.2	1.6 ± 0.2	63.1 ± 0.9	2.5

<sup>a</sup>Values presented are an average of three replicates. <sup>b</sup>Total activity. Activities of all mutant enzymes relative to that of the wild-type enzyme (100%; 103.4  $\mu\text{mol}/\text{min}/\text{mg}$ ). Enzyme activity was measured in triplicate experiments with 10% (w/w) lactose at 40 °C. <sup>c</sup>Wild-type and mutant enzymes (3.75U of each) were incubated with 50% (w/w) lactose, at 60 °C for 20 h. Yields are expressed as grams of product obtained from 100 g initial lactose. A calibration curve of structure 12 ( $\beta$ -D-Galp-(1  $\rightarrow$  3)- $\beta$ -D-Galp-(1  $\rightarrow$  4)-D-Glcp) ranging from 4 to 200  $\mu\text{g}/\text{mL}$  was used for its quantification. <sup>d</sup>Yields are expressed as grams of GOS produced from 100 g initial lactose. Calibration curves for lactose, galactose and glucose, ranging from 10 to 1000  $\mu\text{M}$ , were used for quantification. <sup>e</sup>This is the percentage (%) of structure 12 in total GOS.

10 other compounds were completely novel structures ([Figure 3B](#)).

Mutations of residue R484 greatly altered the enzyme activity and GOS linkage specificity. The activity of all mutants decreased compared to the wild-type BgaD-D enzyme ([Table 2](#)). The largest decrease was caused by the substitution of arginine to tryptophan; this mutant enzyme retained only 17.9% activity compared to the wild-type enzyme. Mutants R484S, R484H, R484G, R584N, R484Q retained about half of their activity. The GOS yields of the mutant enzymes were comparable to that of the wild-type enzyme ([Table 2](#)). The wild-type BgaD-D and R484 mutant enzymes respectively produced 63.5 g and 57.9–66.4 g of GOS from 100 g of initial lactose when incubated at 60 °C for 20 h ([Table 2](#)).

In the product mixture of the wild-type enzyme, only a trace amount of the trisaccharide  $\beta$ -D-Galp-(1  $\rightarrow$  3)- $\beta$ -D-Galp-(1  $\rightarrow$  4)-D-Glcp (Structure 12) is present, i.e., 0.2 g from 100 g of lactose ([Table 2](#)). In contrast, all mutants showed significantly increased yields of this compound. The highest yield (more than 50 times) was achieved with R484S (10.5 g), followed by R484H (10.2 g), R484G (8.7 g), and R484N (8.5 g). In fact, structure 12 became one of the most abundant compounds in the GOS mixture produced by these mutants after 20 h of

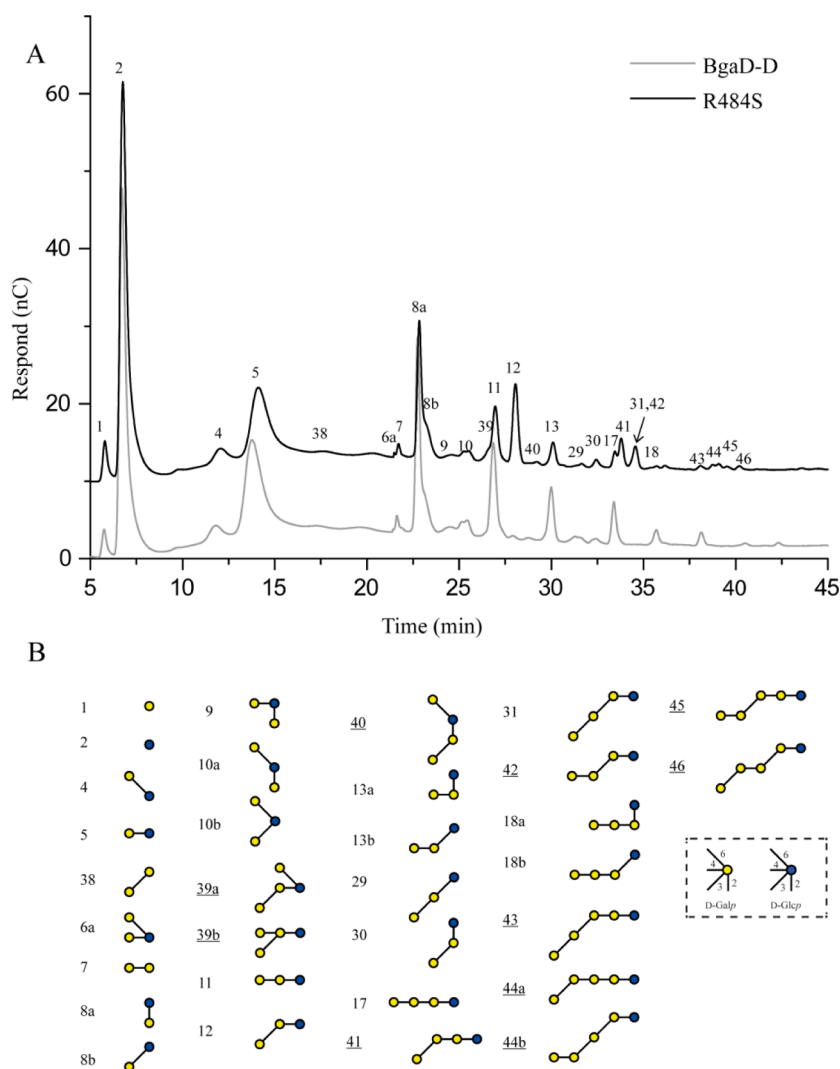


**Figure 3.** (A) HPAEC-PAD analysis of the galacto-oligosaccharides synthesized by the wild-type BgaD-D and R484S mutant using 50% (w/w) lactose as substrate (B) GOS structures<sup>37,38</sup> identified in the R484S mutant product mixture, corresponding to the peak numbers in (A). The numbers of the novel structures are shown underlined.

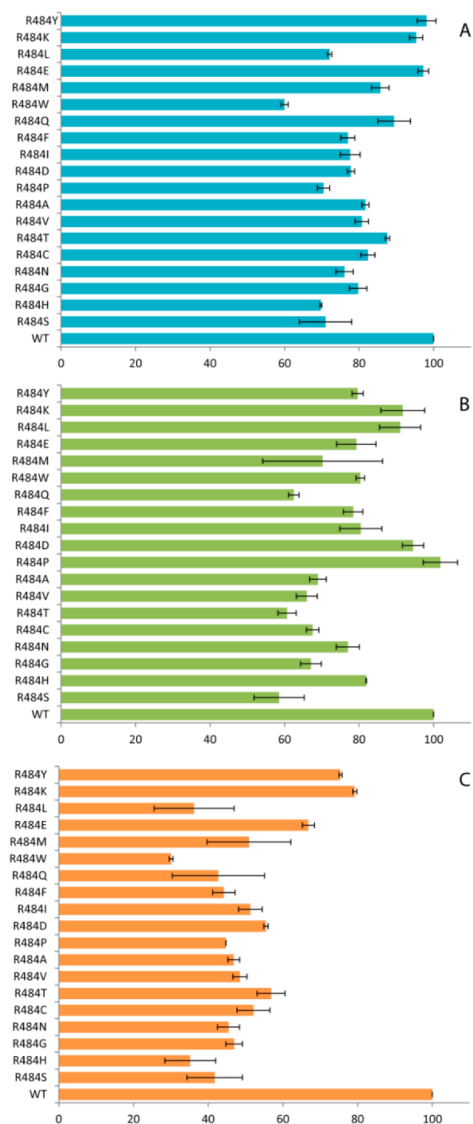
incubation; e.g., it represents 16.9% of the GOS mixture produced by mutant R484H (Table 2).

Figure 4 shows the relative yields of main GOS structures produced by BgaD-D mutants, with respect to that of the wild-type enzyme. According to the peak intensity shown in Figure 3, peak 8 ( $\beta$ -D-Galp-(1  $\rightarrow$  3)- $\beta$ -D-Glcp and  $\beta$ -D-Galp-(1  $\rightarrow$  2)- $\beta$ -D-Glcp), peak 11 ( $\beta$ -D-Galp-(1  $\rightarrow$  4)- $\beta$ -D-Galp-(1  $\rightarrow$  4)-D-Glcp), and peak 13 ( $\beta$ -D-Galp-(1  $\rightarrow$  4)- $\beta$ -D-Galp-(1  $\rightarrow$  3)-D-Glcp and  $\beta$ -D-Galp-(1  $\rightarrow$  4)- $\beta$ -D-Galp-(1  $\rightarrow$  2)-D-Glcp) are the major structures in the GOS produced by the wild-type enzyme. For each mutant, the relative yield of these structures decreased (Figure 4). For example, mutant R484W only produced 60.0% of disaccharide 8 (Figure 4A). The relative yield of trisaccharide 11 decreased to 58.5% for mutant R484S (Figure 4B). Mutant R484W had a relative yield of only 30.1% for trisaccharides 13a and 13b (Figure 4C). Notably, mutants producing high amounts of 12 (R484S, R484H, R484G, R484N) (Table 2) decreased significantly in the yield of these structures (Figure 4).

## DISCUSSION

The structural and linkage variability of GOS is far lower than that of hMOS,<sup>28</sup> while this structural diversity is considered as the basis for their multiple biological functions.<sup>29</sup> More detailed studies of GOS structure and functionality revealed that GOS with different linkages have different prebiotic effects and selectivity toward colonic bacteria.<sup>39–41</sup> Synthesis of GOS with new structures thus has the potential to enhance the functionality of GOS mixtures.

Enzyme engineering has been used as an approach to optimize properties of the  $\beta$ -galactosidase enzyme<sup>42</sup> and to modulate the production of GOS with respect to transglycosylation efficiency and product size. For example, deletion mutagenesis showed that removal of 580 amino acids from the C-terminus of  $\beta$ -galactosidase from *Bifidobacterium bifidum* greatly improved its transgalactosylation ability.<sup>43</sup> The native enzyme only has transgalactosylation activity at high lactose concentration, while the truncated enzyme has a relatively high yield of GOS (39%) even at only 10% initial lactose.<sup>43</sup> A single mutation (F426Y) in  $\beta$ -glucosidase from *Pyrococcus furiosus* increased the transglycosylation and hydrolysis ratio, increasing the GOS yield from 40% to 45%. A double mutant (F426Y/



**Figure 4.** Effects of mutations in residue R484 on the yield of (A) structures **8a** and **8b**, (B) structure **11**, (C) structures **13a** and **13b**, relative to wild-type (WT, 100%).

M424 K) improved GOS synthesis at 10% lactose from 18% to 40%.<sup>44</sup> A mutagenesis approach was also applied to  $\beta$ -galactosidase from *Geobacillus stearothermophilus*; mutation R109W increased the yield of trisaccharide  $\beta$ -D-Galp-(1  $\rightarrow$  3)- $\beta$ -D-Galp-(1  $\rightarrow$  4)-D-Glcp from 2% to 23% at a lactose concentration of 18%.<sup>45</sup> Double mutants of F571L/N574S and F571L/N574A of *Thermotoga maritima*  $\beta$ -Galactosidase increased yield of the major GOS compound  $\beta$ -D-Galp-(1  $\rightarrow$  3)- $\beta$ -D-Galp-(1  $\rightarrow$  4)-D-Glcp 2-fold.<sup>46</sup> In another mutagenesis study of  $\beta$ -galactosidase from *Sulfolobus solfataricus*, the GOS yield was enhanced by 11% by mutating phenylalanine to tyrosine (F441Y).<sup>47</sup>

Finally, a recent study showed that the use of monoclonal antibodies, synthetic binding peptides which can modulate the catalytic properties of enzymes, altered the enzyme specificity of BgaD-D such that it barely produced any GOS higher than DP5,<sup>48</sup> although no changes in linkage types and no new structures were observed.

Thus, although enzyme engineering of  $\beta$ -galactosidases successfully enhanced the transgalactosylation activity or

limited product diversity, none of these studies focused on changing the enzyme product linkage specificity.

In our study, mutagenesis of R484 in BgaD-D altered the enzyme product linkage specificity, resulting in clearly different GOS product compositions. A detailed structural analysis revealed that entirely new GOS compounds were synthesized, greatly enriching the product diversity. In contrast to the wild-type BgaD-D, which has a clear preference for ( $\beta$ 1  $\rightarrow$  4) linkages, the R484 mutants prefer synthesis of both ( $\beta$ 1  $\rightarrow$  3) and ( $\beta$ 1  $\rightarrow$  4) linkages. In addition, this dual preference results in the synthesis of new GOS structures containing alternating ( $\beta$ 1  $\rightarrow$  3) and ( $\beta$ 1  $\rightarrow$  4) linkages. The possible formation routes for all observed product structures are summarized in Figure S3. This reveals that the new mutant R484S activity allows ( $\beta$ 1  $\rightarrow$  3) elongation to occur irrespective of the previous bond, except for ( $\beta$ 1  $\rightarrow$  6). Structures **39a** and **40** are ( $\beta$ 1  $\rightarrow$  3) elongations of **6a** and **10a**, respectively. In both cases the  $\beta$ -D-Galp-(1  $\rightarrow$  4)- residue is elongated, but not the  $\beta$ -D-Galp-(1  $\rightarrow$  6)- residue. Structures **11** and **12** were found elongated by ( $\beta$ 1  $\rightarrow$  3), as seen in **41** and **31**, respectively. Also ( $\beta$ 1  $\rightarrow$  4) elongation was observed for structures **11** and **12**, seen in **17** and **42**, respectively. Structures **43–46** are the results of further elongations by ( $\beta$ 1  $\rightarrow$  3) and ( $\beta$ 1  $\rightarrow$  4) of structures **17**, **31**, **41**, **42**. Structure **39b** results from a novel activity, resulting in a 3,4-disubstituted galactose residue. Whether this is the result of a ( $\beta$ 1  $\rightarrow$  3)-branching of **11**, or a ( $\beta$ 1  $\rightarrow$  4)-branching of **12**, or the result of both routes, cannot be determined from the available data. A total of 14 new GOS structures were produced by the R484S mutant compared to the wild-type enzyme. Among these, 4 structures are also present in other commercial GOS products,<sup>27</sup> but 10 structures have not been reported before. These new compounds further enrich the composition and variety of available GOS structures.

Interestingly, while mutation of R484 affected the GOS composition and variety, it hardly affected the total amount of GOS produced. As a consequence, the increased yield of trisaccharide **12**, as well as the formation of new structures, occurs at the expense of other structures. For example, for mutant R484S, the yield of **12** increased more than 50 times (from 0.2 to 10.5 g). At the same time, however, the yield of **8** decreased about 30%. The yield of **11** decreased about 42%, and the yield of **13** decreased 58%, as a consequence of formation of **29** and **30**. This may also be the cause that of the 43 structures found for the wild-type enzyme, only 19 were still found in detectable levels, whereas the enzyme activity still allows for the synthesis of all 43 structures.

The effect of mutation of residue R484 on transgalactosylation linkage specificity can be explained by the fact that this residue is located near acceptor subsite +1 of the catalytic site (Figure 2). Given the ( $\beta$ 1  $\rightarrow$  4) linkage specificity of wild-type BgaD-D, acceptor molecules such as lactose preferentially bind in a way that the 4-OH group of the sugar moiety in subsite +1 is positioned to attack the C1 atom of the covalent galactosyl-enzyme intermediate. Mutation of R484 to serine or histidine likely affects the binding mode of lactose (and of other acceptors) such that both the 3-OH and 4-OH of the sugar moiety in subsite +1 can be in a favorable position for the transglycosylation reaction. Apparently, the mutations also affected the catalytic efficiency (Table 1) and led to a lower activity. However, the GOS yields of the mutations were comparable to that of the wild-type enzyme (Table 2).



## CONCLUSIONS AND PERSPECTIVES

Our study shows that mutation of residue R484 significantly alters the product linkage specificity of the *B. circulans*  $\beta$ -galactosidase BgaD-D, resulting in a new GOS mixture composition. In particular, the mutant enzymes synthesized a large amount of GOS with ( $\beta 1 \rightarrow 3$ ) and ( $\beta 1 \rightarrow 4$ ) linkages, of which many are different from all known commercial GOS products.<sup>27</sup> To our knowledge, this is the first paper showing that  $\beta$ -galactosidase enzyme engineering results in a clear change in linkage specificity, yielding an enhanced structural diversity of the GOS produced. The mutant enzymes may find industrial application, depending on the functionality of the GOS produced, which remains to be determined in future work.

## ASSOCIATED CONTENT

### Supporting Information

The Supporting Information is available free of charge on the ACS Publications website at DOI: 10.1021/acs.biochem.7b00032.

The NMR analysis and additional figures (PDF)

## AUTHOR INFORMATION

### Corresponding Author

\*E-mail: l.dijkhuizen@rug.nl

### Notes

The authors declare no competing financial interest.

## ACKNOWLEDGMENTS

This work was funded by the China Scholarship Council (to H.Y.) and by the University of Groningen (to S.S.v.L., L.D., T.P., and X.M.). We also thank Prof. Johannes P. Kamerling for stimulating discussions.

## REFERENCES

- (1) Gibson, G. R., and Roberfroid, M. B. (1995) Dietary modulation of the human colonic microbiota: introducing the concept of prebiotics. *J. Nutr.* 125, 1401–1412.
- (2) Park, A. R., and Oh, D. K. (2010) Galacto-oligosaccharide production using microbial  $\beta$ -galactosidase: current state and perspectives. *Appl. Microbiol. Biotechnol.* 85, 1279–1286.
- (3) Boehm, G., Fanaro, S., Jelinek, J., Stahl, B., and Marini, A. (2003) Prebiotic concept for infant nutrition. *Acta Paediatr.* 92, 64–67.
- (4) Boehm, G., Stahl, B., Jelinek, J., Knol, J., Miniello, V., and Moro, G. E. (2005) Prebiotic carbohydrates in human milk and formulas. *Acta Paediatr.* 94, 18–21.
- (5) Oozeer, R., van Limpt, K., Ludwig, T., Amor, K. B., Martin, R., Wind, R. D., Boehm, G., and Knol, J. (2013) Intestinal microbiology in early life: specific prebiotics can have similar functionalities as human-milk oligosaccharides. *Am. J. Clin. Nutr.* 98, 561S–571S.
- (6) Gourbeyre, P., Denery, S., and Bodinier, M. (2011) Probiotics, prebiotics, and synbiotics: impact on the gut immune system and allergic reactions. *J. Leukocyte Biol.* 89, 685–695.
- (7) Knol, J., Scholtens, P., Kafka, C., Steenbakkers, J., Groß, S., Helm, K., Klarczyk, M., Schöpfer, H., Böckler, H.-M., and Wells, J. (2005) Colon microflora in infants fed formula with galacto- and fructo-oligosaccharides: more like breast-fed infants. *J. Pediatr. Gastroenterol. Nutr.* 40 (1), 36–42.
- (8) Monteagudo-Mera, A., Arthur, J. C., Jobin, C., Keku, T., Bruno-Barcena, J. M., and Azcarate-Peril, M. A. (2016) High purity galacto-oligosaccharides enhance specific *Bifidobacterium* species and their metabolic activity in the mouse gut microbiome. *Benefic. Microbes* 7, 247–264.

- (9) Arslanoglu, S., Moro, G. E., Schmitt, J., Tandoi, L., Rizzardi, S., and Boehm, G. (2008) Early dietary intervention with a mixture of prebiotic oligosaccharides reduces the incidence of allergic manifestations and infections during the first two years of life. *J. Nutr.* 138, 1091–1095.

- (10) Van Hoffen, E., Ruiters, B., Faber, J., M'Rabet, L., Knol, E. F., Stahl, B., Arslanoglu, S., Moro, G., Boehm, G., and Garssen, J. (2009) A specific mixture of short-chain galacto-oligosaccharides and long-chain fructo-oligosaccharides induces a beneficial immunoglobulin profile in infants at high risk for allergy. *Allergy* 64, 484–487.

- (11) Shoaf, K., Mulvey, G. L., Armstrong, G. D., and Hutkins, R. W. (2006) Prebiotic galactooligosaccharides reduce adherence of enteropathogenic *Escherichia coli* to tissue culture cells. *Infect. Immun.* 74, 6920–6928.

- (12) Vulevic, J., Drakoularakou, A., Yaqoob, P., Tzortzis, G., and Gibson, G. R. (2008) Modulation of the fecal microflora profile and immune function by a novel trans-galactooligosaccharide mixture (B-GOS) in healthy elderly volunteers. *Am. J. Clin. Nutr.* 88, 1438–1446.

- (13) Tremaroli, V., and Bäckhed, F. (2012) Functional interactions between the gut microbiota and host metabolism. *Nature* 489, 242–249.

- (14) Playne, M. J., and Crittenden, R. G. (2009) Galacto-oligosaccharides and other products derived from lactose. *Adv. Dairy Chem.* 3, 121–202.

- (15) Sanz, M. L., Sanz, J., and Martínez-Castro, I. (2002) Characterization of O-trimethylsilyl oximes of disaccharides by gas chromatography-mass spectrometry. *Chromatographia* 56, 617–622.

- (16) Yin, H., Bultema, J. B., Dijkhuizen, L., and van Leeuwen, S. S. (2017) Reaction kinetics and galactooligosaccharide product profiles of the  $\beta$ -galactosidases from *Bacillus circulans*, *Kluyveromyces lactis* and *Aspergillus oryzae*. *Food Chem.* 225, 230.

- (17) Bultema, J. B., Kuipers, B. J. H., and Dijkhuizen, L. (2014) Biochemical characterization of mutants in the active site residues of the  $\beta$ -galactosidase enzyme of *Bacillus circulans* ATCC 31382. *FEBS Open Bio* 4, 1015–1020.

- (18) Juers, D. H., Matthews, B. W., and Huber, R. E. (2012) *LacZ*  $\beta$ -galactosidase: structure and function of an enzyme of historical and molecular biological importance. *Protein Sci.* 21, 1792–1807.

- (19) Torres, D. P. M., Gonçalves, M. d. P. F., Teixeira, J. A., and Rodrigues, L. R. (2010) Galacto-oligosaccharides: production, properties, applications, and significance as prebiotics. *Compr. Rev. Food Sci. Food Saf.* 9, 438–454.

- (20) Otieno, D. O. (2010) Synthesis of  $\beta$ -galactooligosaccharides from lactose using microbial  $\beta$ -galactosidases. *Compr. Rev. Food Sci. Food Saf.* 9, 471–482.

- (21) Gosling, A., Stevens, G. W., Barber, A. R., Kentish, S. E., and Gras, S. L. (2010) Recent advances refining galactooligosaccharide production from lactose. *Food Chem.* 121, 307–318.

- (22) Rodriguez-Colinas, B., de Abreu, M. A., Fernandez-Arrojo, L., de Beer, R., Poveda, A., Jimenez-Barbero, J., Haltrich, D., Ballesteros Olmo, A. O., Fernandez-Lobato, M., and Plou, F. J. (2011) Production of galacto-oligosaccharides by the  $\beta$ -galactosidase from *Kluyveromyces lactis*: comparative analysis of permeabilized cells versus soluble enzyme. *J. Agric. Food Chem.* 59, 10477–10484.

- (23) Urrutia, P., Rodriguez-Colinas, B., Fernandez-Arrojo, L., Ballesteros, A. O., Wilson, L., Plou, F. J., and Illanes, A. (2013) Detailed analysis of galactooligosaccharides synthesis with  $\beta$ -galactosidase from *Aspergillus oryzae*. *J. Agric. Food Chem.* 61, 1081–1087.

- (24) Yanahira, S., Kobayashi, T., Suguri, T., Nakakoshi, M., Miura, S., Ishikawa, H., and Nakajima, I. (1995) Formation of oligosaccharides from lactose by *Bacillus circulans*  $\beta$ -galactosidase. *Biosci., Biotechnol., Biochem.* 59, 1021–1026.

- (25) van Leeuwen, S. S., Kuipers, B. J. H., Dijkhuizen, L., and Kamerling, J. P. (2014) <sup>1</sup>H NMR analysis of the lactose/ $\beta$ -galactosidase-derived galacto-oligosaccharide components of Vivinal® GOS up to DP5. *Carbohydr. Res.* 400, 59–73.

- (26) van Leeuwen, S. S., Kuipers, B. J. H., Dijkhuizen, L., and Kamerling, J. P. (2016) Corrigendum to “<sup>1</sup>H NMR analysis of the

lactose/ $\beta$ -galactosidase-derived galacto-oligosaccharide components of Vivinal® GOS up to DP5" [Carbohydr. Res. 400 (2014) 59–73]. *Carbohydr. Res.* 419, 69–70.

(27) van Leeuwen, S. S., Kuipers, B. J. H., Dijkhuizen, L., and Kamerling, J. P. (2016) Comparative structural characterization of 7 commercial galacto-oligosaccharide (GOS) products. *Carbohydr. Res.* 425, 48–58.

(28) Sela, D. A., and Mills, D. A. (2010) Nursing our microbiota: molecular linkages between bifidobacteria and milk oligosaccharides. *Trends Microbiol.* 18, 298–307.

(29) Barile, D., and Rastall, R. A. (2013) Human milk and related oligosaccharides as prebiotics. *Curr. Opin. Biotechnol.* 24, 214–219.

(30) Kralj, S., van Geel-Schutten, I. G. H., Faber, E. J., van der Maarel, M. J. E. C., and Dijkhuizen, L. (2005) Rational transformation of *Lactobacillus reuteri* 121 reuteransucrase into a dextranucrase. *Biochemistry* 44, 9206–9216.

(31) Meng, X., Dobruchowska, J. M., Pijning, T., López, C. A., Kamerling, J. P., and Dijkhuizen, L. (2014) Residue Leu<sup>940</sup> has a crucial role in the linkage and reaction specificity of the glucanucrase GTF180 of the probiotic bacterium *Lactobacillus reuteri* 180. *J. Biol. Chem.* 289, 32773–32782.

(32) Ishikawa, K., Kataoka, M., Yanamoto, T., Nakabayashi, M., Watanabe, M., Ishihara, S., and Yamaguchi, S. (2015) Crystal structure of  $\beta$ -galactosidase from *Bacillus circulans* ATCC 31382 (BgaD) and the construction of the thermophilic mutants. *FEBS J.* 282, 2540–2552.

(33) Singh, A. K., Pluinage, B., Higgins, M. A., Dalia, A. B., Woodiga, S. A., Flynn, M., Lloyd, A. R., Weiser, J. N., Stubbs, K. A., Boraston, A. B., and King, S. J. (2014) Unravelling the multiple functions of the architecturally intricate BgaA. *PLoS Pathog.* 10, e1004364.

(34) Song, J., Abe, K., Imanaka, H., Imamura, K., Minoda, M., Yamaguchi, S., and Nakanishi, K. (2011) Causes of the production of multiple forms of  $\beta$ -galactosidase by *Bacillus circulans*. *Biosci., Biotechnol., Biochem.* 75, 268–278.

(35) Song, J., Imanaka, H., Imamura, K., Minoda, M., Yamaguchi, S., and Nakanishi, K. (2013) The discoidin domain of *Bacillus circulans*  $\beta$ -galactosidase plays an essential role in repressing galactooligosaccharide production. *Biosci., Biotechnol., Biochem.* 77, 73–79.

(36) van Leeuwen, S. S., Kuipers, B. J. H., Dijkhuizen, L., and Kamerling, J. P. (2014) Development of a <sup>1</sup>H NMR structural-reporter-group concept for the analysis of prebiotic galacto-oligosaccharides of the [ $\beta$ -D-Galp-(1→x)]<sub>n</sub>-D-Glcp type. *Carbohydr. Res.* 400, 54–58.

(37) Ceroni, A., Maass, K., Geyer, H., Geyer, R., Dell, A., and Haslam, S. M. (2008) Glycoworkbench: a tool for the computer-assisted annotation of mass spectra of glycans. *J. Proteome Res.* 7, 1650–1659.

(38) Perez, S. (2014) *Symbolic Representation of Monosaccharides in the Age of Glycobiology*, p 119, [www.Glycopedia.Eu](http://www.Glycopedia.Eu)

(39) Depeint, F., Tzortzis, G., Vulevic, J., I'Anson, K., and Gibson, G. R. (2008) Prebiotic evaluation of a novel galactooligosaccharide mixture produced by the enzymatic activity of *Bifidobacterium bifidum* NCIMB 41171, in healthy humans: a randomized, double-blind, crossover, placebo-controlled intervention study. *Am. J. Clin. Nutr.* 87, 785–791.

(40) Cardelle-Cobas, A., Corzo, N., Olano, A., Peláez, C., Requena, T., and Ávila, M. (2011) Galactooligosaccharides derived from lactose and lactulose: influence of structure on *Lactobacillus*, *Streptococcus* and *Bifidobacterium* growth. *Int. J. Food Microbiol.* 149, 81–87.

(41) Li, W., Wang, K., Sun, Y., Ye, H., Hu, B., and Zeng, X. (2015) Influences of structures of galactooligosaccharides and fructooligosaccharides on the fermentation in vitro by human intestinal microbiota. *J. Funct. Foods* 13, 158–168.

(42) Quin, M. B., and Schmidt-Dannert, C. (2011) Engineering of biocatalyst from evolution to creation. *ACS Catal.* 1, 1017–1021.

(43) Jørgensen, F., Hansen, O. C., and Stougaard, P. (2001) High-efficiency synthesis of oligosaccharides with a truncated  $\beta$ -galactosidase from *Bifidobacterium bifidum*. *Appl. Microbiol. Biotechnol.* 57, 647–652.

(44) Hansson, T., Kaper, T., van der Oost, J., de Vos, W. M., and Adlercreutz, P. (2001) Improved oligosaccharide synthesis by protein

engineering of beta-glucosidase CelB from hyperthermophilic *Pyrococcus furiosus*. *Biotechnol. Bioeng.* 73, 203–210.

(45) Placier, G., Watzlawick, H., Babilier, C., and Mattes, R. (2009) Evolved  $\beta$ -galactosidases from *Geobacillus stearothermophilus* with improved transgalactosylation yield for galacto-oligosaccharide production. *Appl. Environ. Microbiol.* 75, 6312–6321.

(46) Talens-Perales, D., Polaina, J., and Marín-Navarro, J. (2016) Structural dissection of the active site of *Thermotoga maritima*  $\beta$ -Galactosidase identifies key residues for transglycosylating activity. *J. Agric. Food Chem.* 64, 2917–2924.

(47) Wu, Y., Yuan, S., Chen, S., Wu, D., Chen, J., and Wu, J. (2013) Enhancing the production of galacto-oligosaccharides by mutagenesis of *Sulfolobus solfataricus*  $\beta$ -galactosidase. *Food Chem.* 138, 1588–1595.

(48) Tanaka, S., Takahashi, T., Koide, A., Ishihara, S., Koikeda, S., and Koide, S. (2015) Monobody-mediated alteration of enzyme specificity. *Nat. Chem. Biol.* 11, 762–764.